

## Purpose

MRI guided radiotherapy (MRIgRT) is an emerging technology which directly translates to having a proficient auditing beam system for such devices. A patient whom is expected to receive therapy on a MRIgRT device will first obtain a CT, which will be used to perform a treatment plan. During treatment, on a MRIgRT device, real time images can be acquired on the MR unit for target localization.<sup>1-2</sup>

MR and CT acquire images very differently. CT measures electron density; whereas, the rate at which the proton, in the hydrogen nuclei, relaxes back to equilibrium is used to produce a MR signal.<sup>3-5</sup> The main purpose of this study is to identify lung, soft tissue, and tumor mimicking substitutes that share similar human-like CT and MR properties (i.e. Hounsfield units and relaxation times) which could further be used to manufacture a heterogeneous anthropomorphic End to End QA phantom.

## Motivation for this study

- Due to different principles in which MR and CT acquire images, some materials are not visualized on both modalities.
- Compress cork is typically used as lung-equivalent material in RPC thoracic anthropomorphic phantoms; however, as shown in Fig.1 and Fig. 2, in a T1-weighted image from a 1.5T GE Signa HDx Scanner, the 2.5 x 2.5 x 2.5cm<sup>3</sup> compress cork cube is not visualized.
- Some materials that were imaged in both GE Discovery 750HD CT, and a 1.5T GE Signa HDx Scanners could only be visualized in CT and T1-weighted images and were not observed in T2-weighted images. (Fig. 3 & 4)

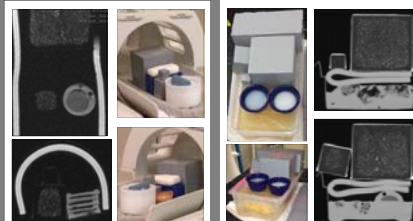


Figure 1: Material of interest were first scanned on a GE 1.5T Signa HDx Scanner. Some tested materials (smaller compressed cork, epoxy resin, machinable wax, paraffin/hellof calcium carbonate, and titanium dioxide/machinable wax) were not visible on T1-weighted images.

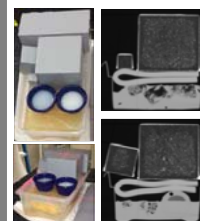


Figure 2: Materials imaged on a GE Lightspeed RT16 CT simulator. There were three different compress cork sizes seal with water. The smallest compress cork appeared to have no water sealed, where the middle and large size compress cork cubes showed irregular profiles of water.



Figure 3: Material of interest, polyurethane sponge saturated in water, and SmoothOn products: ReoFlex 30 & 20, Vyal Flex 30 & 20, PMC 121/30, Dragon Skin, EcoFlex 30 were scanned on a GE 1.5T Signa HDx Scanner T1 (Left) and T2 (right) weighted images were acquired. SmoothOn's ReoFlex 30 & 20, Vyal Flex 30 & 20, PMC 121/30 were not visible on T2.

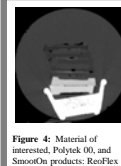


Figure 4: Material of interest, Polytek 00, and SmoothOn products: ReoFlex 30 & 20, Vyal Flex 30 & 20, PMC 121/30, Dragon Skin, EcoFlex 30 were scanned on GE Discovery 750HD CT and HU were measured.

## Method

Common CT QA phantom materials, and other proprietary gels/silicones from Polytek, SmoothOn, and CompositeOne were first scanned on a GE 1.5T Signa HDxT MR to test how visible they were on T1 and T2 weighted images. Average HU values were measured on both GE Lightspeed RT16 CT simulator and GE Discovery 750HD CT scanner. Materials with matching HU values of lung (-500 to -700HU), muscle (+40HU) and soft tissue (+100 to +300HU) were further scanned on GE 1.5T Signa HDx to measure their T1 and T2 relaxation times.

T1 was measured by applying a single slice inversion recovery spin echo sequence and varying inversion time (TI) by: 50, 100, 200, 400, 800, 1600, and 2900ms while the repetition time (TR) remain constant.<sup>6</sup> T2 was measured by applying the 2D spin-echo sequence and varying the echo time (TE) by: 10, 20, 30, 40, 60, 80, 160, and 320 ms.<sup>6</sup> Through Matlab, ROI were denoted and the average signal was measured in each material. The Levenberg-Marquardt least-squares algorithm was then applied to Eq. 1 and Eq. 2 (where M<sub>0</sub> represents the equilibrium magnetization, and S is the average signal) to measure T1 and T2, respectively.

$$S = M_0 \left( 1 - 2e^{-\frac{TI}{T_1}} + e^{-\frac{TR}{T_1}} \right) \quad (Eq. 1)$$

$$S = M_0 e^{-\frac{TE}{T_2}} \quad (Eq. 2)$$

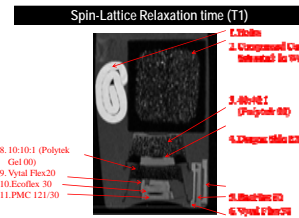


Figure 4a: Materials of interest imaged on a 1.5T GE Signa HDx scanner and used 3DFSPGR (T1) sequence.

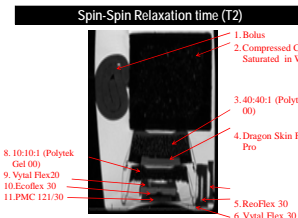


Figure 4b: Materials of interest imaged on a 1.5T GE Signa HDx scanner and used F1ESTA (T2) sequence.

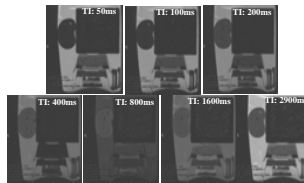


Figure 4c: Materials of interest imaged on a 1.5T GE Signa HDx scanner and T1 values were measured by varying TI.

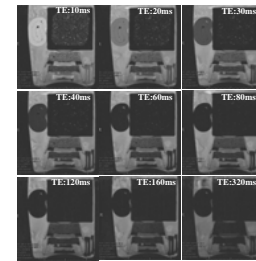


Figure 4d: Materials of interest imaged on a 1.5T GE Signa HDx scanner and T2 values were measured by varying TE.

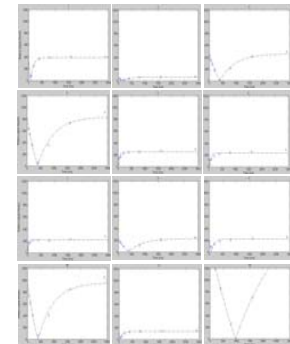


Figure 4e: Graphical representation of T1 relaxation rates from the materials of interest.

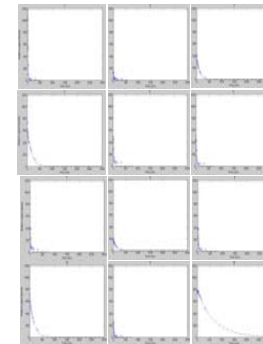
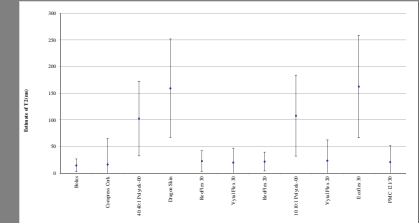
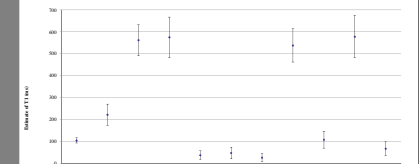


Figure 4f: Graphical representation of T2 relaxation rates from the materials of interest.

## Results

Parameters	T1 (1.5T)		T2 (1.5T)		Average HU
	TI (ms)	T2 (ms)	TE (ms)	T2 (ms)	
Sequence	Single slice inversion recovery spin echo	2D Spin Echo			
Matrix Size	128x128	128x128			
NEX	0.5	1			
FOV (mm)	240.0	240.0			
TE (ms)	28.84	10, 20, 30, 40, 60, 80, 160, 320			
TR (ms)	3000	1000			
T1 (ms)	50, 100, 200, 400, 800, 1600, 2900	0			
Material					
Bolus		104.2	14.29	-59.5	
Compress Cork		221.6	16.14	-646.7	
40:40:1 Polytek Gel 00		561.8	102.4	-360	
Dragon Skin FX Pro		575.0	159.4	199.5	
ReoFlex 30		37.1	22.45	-22.5	
Vyal Flex 20		46.8	19.85	-13.5	
ReoFlex 20		26.1	21.50	-19.5	
10:10:1 Polytek Gel 00		537.8	107.9	-680	
Vyal Flex 20		107.4	23.26	-18	
Ecoflex 00-30		578.4	162.4	182.5	
PMC 121/30		66.6	20.77	-11	
Water		1917	820.8	0	



## Conclusion

- Mini styrofoam balls combined with different concentrations of Polytek-00 [Polytek10g of A, 10g of B and 1 g of styrofoam balls and Polytek 40g of A, 40g of B and 1 g of styrofoam balls] can modify HU and change hydrogen content of each mixture; thus, vary T1 and T2 relaxation times.
- Compressed cork saturated with water, Polytek-00 combined with mini styrofoam balls was examined for lung equivalent material.
- Bolus, SmoothOn's Dragon-Skin and Ecoflex could potentially be used for soft tissue and tumor equivalent material.

## References

1. Mutic, S., & Dempsey, J. F. (2014, July). The ViewRay System: Magnetic Resonance-Guided and Controlled Radiotherapy. In *Seminars in radiation oncology* (Vol. 24, No. 3, pp. 196-199). WB Saunders.
2. Raaymakers, B. W., Lagendijk, J. J. W., Overweg, J., Kok, J. G. M., Raaijmakers, A. J. E., Kerkhof, E. M., ... & Brown, K. J. (2009). Integrating a 1.5 T MRI scanner with a 6 MV accelerator: proof of concept. *Physics in medicine and biology*, 54(12), N229.
3. Berger, A. (2002). How does it work? Magnetic resonance imaging. *BMJ: British Medical Journal*, 324(7328), 35.
4. McRobbie, D. (2007). *MRI from picture to proton* (2nd ed.). Cambridge, UK: Cambridge University Press.
5. The Role of Imaging Radiotherapy Treatment Planning. (2001). In S. Stergiopoulos (Ed.), *Advanced Signal Processing Handbook: Theory and Implementation for Radar, Sonar, and Medical Imaging Real-Time Systems*. Boca Raton, FL: CRC Press.
6. Lim, T. Y., Stafford, R. J., Kuchchaker, R. J., Sankaranarayananpillai, M., Ibbott, G., Rao, A., ... & Frank, S. J. (2014). MRI characterization of cobalt dichloride-N-acetyl cysteine (C4) contrast agent marker for prostate brachytherapy. *Physics in medicine and biology*, 59(10), 2505.